

PAPER • OPEN ACCESS

## Dielectric and electromagnetic interference shielding properties of carbon black nanoparticles reinforced PVA/PEG blend nanocomposite films

To cite this article: Priyanka Rani *et al* 2020 *Mater. Res. Express* 7 064008

View the [article online](#) for updates and enhancements.



**IOP | ebooks™**

Bringing together innovative digital publishing with leading authors from the global scientific community.

Start exploring the collection—download the first chapter of every title for free.



## PAPER

# Dielectric and electromagnetic interference shielding properties of carbon black nanoparticles reinforced PVA/PEG blend nanocomposite films

## OPEN ACCESS

RECEIVED  
17 March 2020REVISED  
21 May 2020ACCEPTED FOR PUBLICATION  
1 June 2020PUBLISHED  
10 June 2020

Original content from this work may be used under the terms of the [Creative Commons Attribution 4.0 licence](#).

Any further distribution of this work must maintain attribution to the author(s) and the title of the work, journal citation and DOI.

Priyanka Rani<sup>1</sup>, M Basheer Ahamed<sup>1</sup>  and Kalim Deshmukh<sup>2</sup><sup>1</sup> Department of Physics, B. S. Abdur Rahman Crescent Institute of Science and Technology, Vandalur, Chennai, 600048, Tamil Nadu, India<sup>2</sup> New Technologies—Research Centre, University of West Bohemia, Plzeň, 30100, Czech Republic

†This work was presented at the 2nd International Conference on Nanoscience and Nanotechnology (ICNAN'19) at VIT University, Vellore (India) from 29th Nov - 1st Dec. 2019. Chairman: Prof. A. Nirmala Grace.

E-mail: [basheerahamed@crescent.education](mailto:basheerahamed@crescent.education)**Keywords:** EMI shielding, dielectrics, carbon black nanoparticles, polymer nanocomposites

## Abstract

Polyvinyl alcohol (PVA)/polyethylene glycol (PEG) blend nanocomposite films reinforced with various loadings of carbon black nanoparticles (CBNPs) were synthesized via a solution casting approach. The structural properties of PVA/PEG/CBNPs nanocomposites were investigated using Fourier-transform infrared (FTIR) spectroscopy, indicating the strong interaction of CBNPs with the polymer blend. The thermogravimetric analysis (TGA) and differential scanning calorimetry (DSC) results respectively confirmed the enhanced thermal stability and the variation in the melting temperature with the addition of CBNPs in polymer blend. The dielectric measurements of nanocomposite films were carried out over a frequency range from 50 Hz–20 MHz at a varied temperature range from 40 °C–150 °C using impedance analyzer. The maximum dielectric constant for neat PVA was observed to be about 21.4 at 50 Hz and 150 °C. For PVA/PEG/CBNPs nanocomposites having higher loading of CBNPs (25 wt%) the maximum value of dielectric constant was found to be  $\epsilon = 375.1$  at 50 Hz, 150 °C. The dielectric properties increased with the addition of CBNPs which validates a significant control on percolation threshold attributing to the well-dispersed CBNPs in the polymer blend. The electromagnetic interference (EMI) shielding effectiveness (SE) was improved from 0.1 dB to 10.6 dB with the addition of CBNPs in the PVA/PEG blend. The improved EMI SE and dielectric performance of these nanocomposites suggest CBNPs as excellent nanofillers for the development of flexible, lightweight and low-cost material for electronic applications.

## Introduction

Modern society is concerned with the unwanted electromagnetic interference (EMI) signals that arise due to the evolution in the consumption of industrial, commercial, military, wireless and high-speed communication systems. These EMI signals cause perturbation and distortion in the operation of electronic devices [1, 2]. Therefore, shielding of such electronic devices is necessary to avoid degradation in their performance. In recent years, polymer nanocomposites (PNCs) comprising novel polymeric systems and carbon-based nanofillers have gained much attention for the development of effective, light-weight dielectric and EMI shielding materials [3–7]. Among varied types of polymers, the electrically insulating polymers exhibit very low dielectric constant values leading to poor shielding attenuation, therefore to enhance such property they are reinforced with electrically conducting fillers [1–3, 8]. Several researchers developed advanced conductive nanocomposites by adding various conductive nanofillers as carbon black nanoparticles (CBNPs) [4], carbon nanotubes (CNT) [5], carbon nanofibers (CNF) [6] and metal nanoparticles etc [7]. Furthermore, the interaction between conductive polymer and nanofiller leads to high dielectric constant and low dielectric loss resulting from the insulator–conductor transition occurring near the percolation threshold [8]. To achieve better electrical conductivity, a

higher concentration of metal nanoparticles is needed and as a result composites become heavy and inflexible [9]. On the other hand, CBNPs reinforced PNCs preserves the flexibility of composites and are lightweight, eco-friendly as well as exhibit good thermal stability [10]. CBNPs are being used in various applications, including electronic packaging, protective coatings, storage capacitors, structural reinforcement, EMI shielding, heating elements, and so on [4, 5]. CBNPs exhibits exceptional properties like high specific surface area, conducting nature, varied particle size, strong electric forces which closely bounds the aggregates [11]. CBNPs reinforced PNCs were extensively used in aerospace industries as a flooring material for the dissipation of static electricity charges and the fabrication of modern electrical devices and components [4].

Polyvinyl alcohol (PVA) being a hydrophilic-organic polymer has fascinated the interest of material scientists due to its variety of applications in food packaging, humidity sensors, thin-film transistors, fuel cells, and so on [12, 13]. PVA forms hydrogen bonding with other polymeric matrices due to the presence of hydroxyl groups and exhibits good charge storage capacity, high dielectric strength, high tensile strength along with excellent film-forming properties [14–18]. PVA being an insulating polymer shows poor conducting nature. The conductivity of PVA at room temperature is relatively low, but blending it with polyethyleneglycol (PEG) will improve its conductivity [19]. PEG is a hydrophilic and non-toxic polymer, having tremendous properties like electron acceptor nature, biocompatibility, chain flexibility and a wide range of molecular weight [19]. PEG is widely used to increase the ductility and flexibility of rigid polymers. However, PEG is having a low melting point than PVA which preserves the highly strengthened carbon chain backbone in PVA as compared with the C–O–C backbone in PEG [19, 20]. Thus, the present work deals with the fabricating CBNPs reinforced PVA/PEG blend nanocomposite films with an intent to investigate their structural, morphological, thermal, dielectric and EMI shielding properties. The obtained results demonstrate the suitability of flexible PVA/PEG/CBNPs nanocomposite films for EMI shielding applications.

## Experimental technique

### Materials

Polyvinyl alcohol (PVA) powder having molecular weight 1, 15 000 g mol<sup>-1</sup> and polyethylene glycol (PEG) powder with molecular weight 6000 g mol<sup>-1</sup> were supplied by Loba Chemie Pvt. Ltd Mumbai, India. CBNPs with 21 nm average particle size were procured from Plasma Chem GmbH, Berlin, Germany. Double de-ionized water was utilized as a solvent for the synthesis of CBNPs reinforced PVA/PEG blend nanocomposite films. All the chemicals were used without any further purification.

### Preparation of PVA/PEG/CBNPs Nanocomposite Films

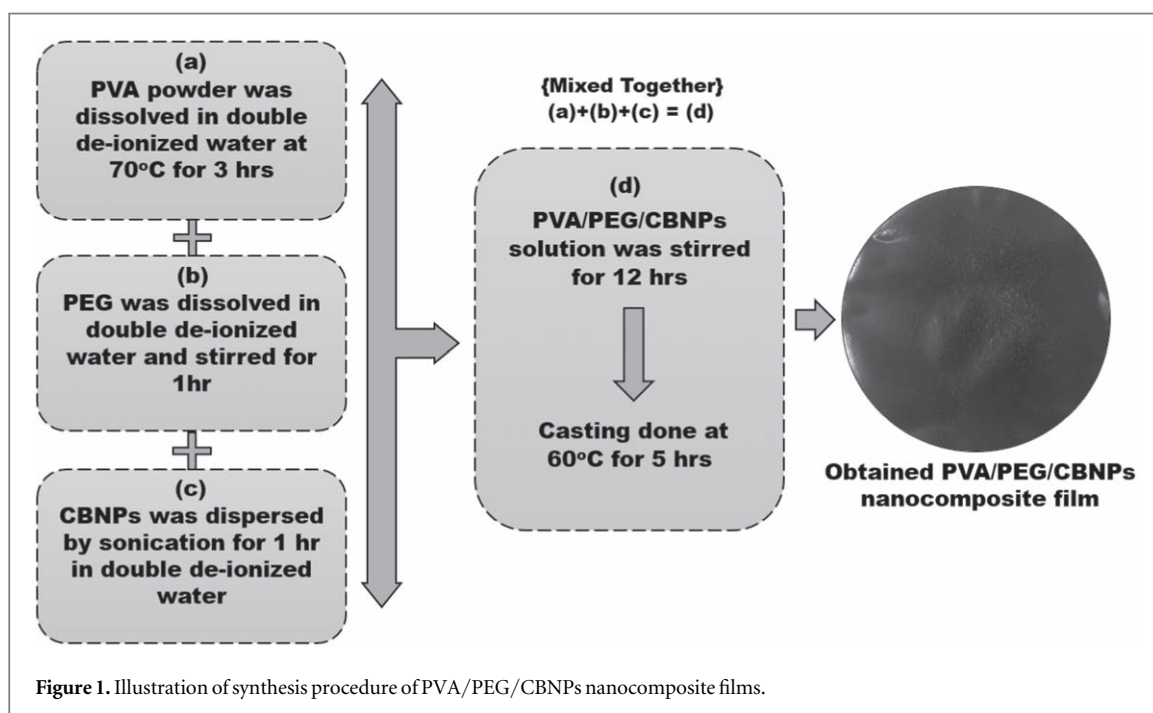
PVA/PEG/CBNPs nanocomposites were synthesized by employing a solvent casting approach using double de-ionized water as a solvent. For the preparation of PVA/PEG blend film, first, 0.75 g of PVA powder was dissolved in 20 ml double deionized water by heating at 70 °C for 3 h in a hot air oven. Later, 0.25 g of PEG powder was dissolved in 20 ml water at room temperature and subsequently added to the prepared PVA solution to form a PVA/PEG blend solution. This blend solution was stirred for 3 hours before casting and drying on Teflon petri dish at 60 °C for 8 hours. After drying, the PVA/PEG blend films were removed from the petri dish and utilized for further study. Similarly, for the preparation of 75/10/15 (wt%) composition of PVA/PEG/CBNPs nanocomposites, 0.75 g of PVA powder was first dissolved in 20 ml double de-ionized water by heating at 70 °C for 3 h in a hot air oven. On the other side, in a separate beaker, 0.10 gm of PEG powder was dissolved in 20 ml solvent at room temperature and subsequently added to the PVA solution. Later, 0.15 gm of CBNPs were dispersed in 20 ml double de-ionized water via ultra-sonication for 1 h at room temperature and then mixed with PVA/PEG blend solution. The obtained homogeneous PVA/PEG/CBNPs dispersion for 75/10/15 (wt%) composition was stirred at room temperature for 8 h and finally spread on a clean Teflon petri dish for drying at 60 °C for 5 h. The resulting PVA/PEG/CBNPs nanocomposite film having a thickness in the range 60–80 μm was peeled off and utilized for further characterizations. The other compositions mentioned in table 1 were also prepared by following the same procedure. The step by step preparation procedure of PVA/PEG/CBNPs nanocomposites is schematically illustrated in figure 1.

## Characterizations

Fourier transform infrared (FTIR) studies of prepared PVA/PEG/CBNPs nanocomposite films with varying content of CBNPs were evaluated using Fourier transform infrared spectrophotometer (Shimadzu, IRAffinity-1, Japan) in a transmittance mode, in wavenumber range from 500 to 4000 cm<sup>-1</sup>.

**Table 1.** Feed composition details of PVA/PEG/CBNPs nanocomposites.

Sr No.	PVA (wt%)	PEG (wt%)	CBNPs (wt%)
1.	75	25	0
2.	75	20	5
3.	75	15	10
4.	75	10	15
5.	75	5	20
6.	75	0	25



Thermal studies of PVA/PEG/CBNPs nanocomposite films with various loadings of CBNPs were evaluated by Shimadzu's TGA-50 series thermogravimetric analyzer (TGA), under nitrogen ( $N_2$ ) atmosphere. The samples were heated up to 800 °C with a rate of 10 °C  $min^{-1}$ .

Differential scanning calorimetry (DSC) measurements of PVA/PEG/CBNPs nanocomposite films with various loadings of CBNPs were carried out using DSC 8000 advanced double furnace differential scanning calorimeter (Perkin Elmer, USA) at a heating rate of 10 °C  $min^{-1}$ , in a temperature range of 10–250 °C, under nitrogen atmosphere.

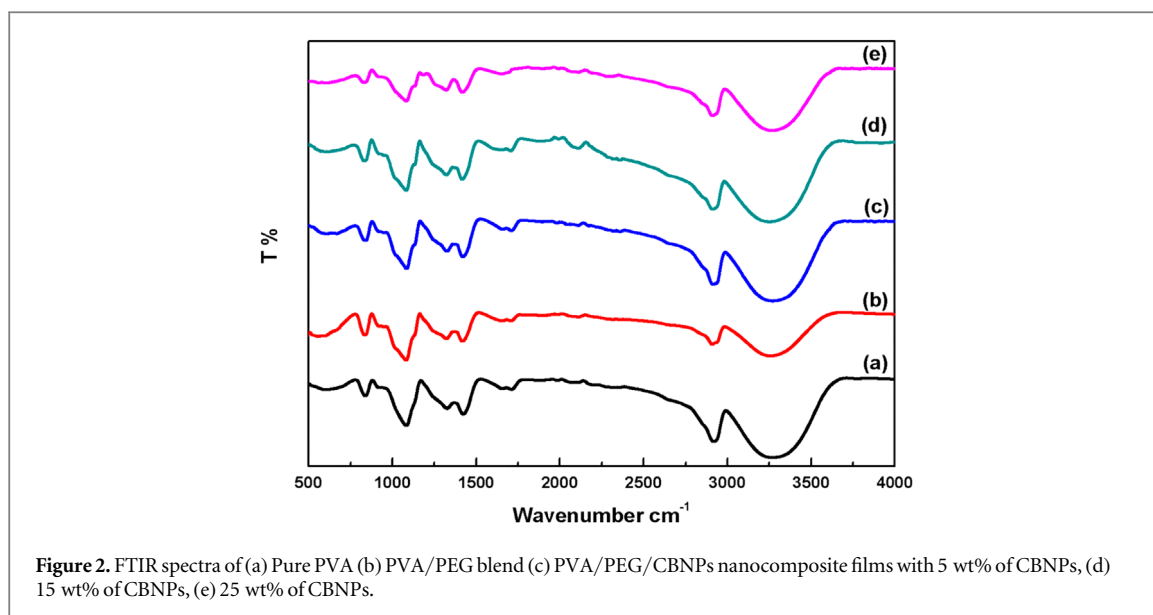
The dielectric measurements of PVA/PEG/CBNPs nanocomposite films with various loadings of CBNPs were evaluated using PSM1735 Impedance Analyser (Newtons 4th Ltd, UK). The samples were coated both sides with silver paste to confirm uniform charge transfer and placed inside the computer controlled-furnace with the accuracy of  $\pm 0.2$  °C. The measurements were carried out at a temperature range (40 °C–150 °C) and in the frequency range (50 Hz–20 MHz).

The EMI SE studies of the PVA/PEG/CBNPs nanocomposite films with various loadings of CBNPs were carried out in the Ku-band frequency region using an 8510C Vector Network Analyzer (VNA), (Agilent Technologies, USA) with a waveguide dimension of 25.5 × 13 × 5.6 mm.

## Results and discussions

### FTIR spectroscopic studies

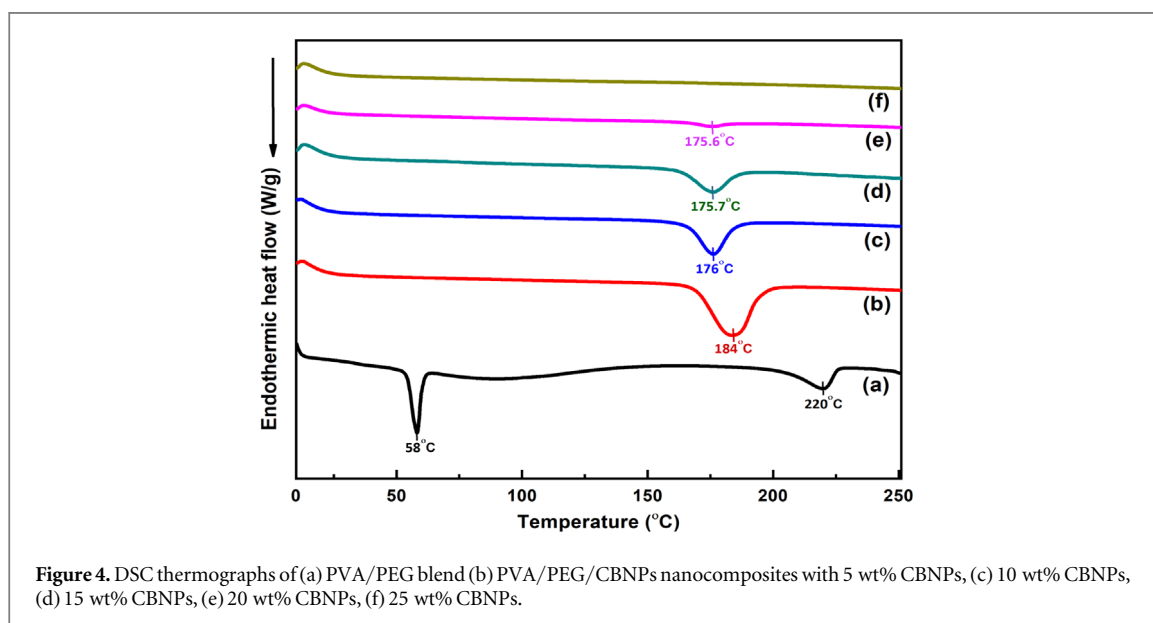
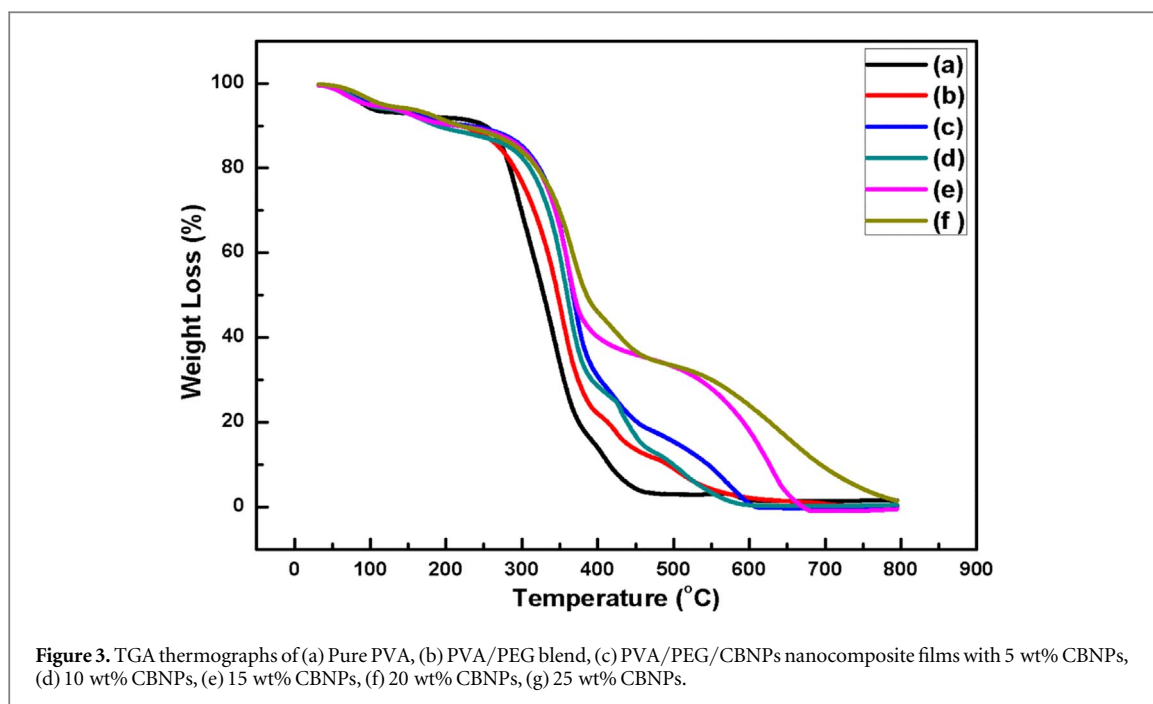
The FTIR spectra of pure PVA and PVA/PEG blend with different loadings of CBNPs are depicted in figures 2(a)–(e). The FTIR spectrum of the neat PVA presented in figure 2(a) shows various characteristic bands. The broad absorption band at 3265  $cm^{-1}$  can be attributed to the vibration of O–H symmetrical stretching [21]. The characteristic peaks at 2939  $cm^{-1}$  and 2908  $cm^{-1}$  can be ascribed to an alkyl group and C–H asymmetric stretching vibration respectively. The absorption band appearing at 1711  $cm^{-1}$  and 1661  $cm^{-1}$  indicates the



C=O stretching vibration of the carbonyl group of PVA [19]. The absorption bands at  $1413\text{ cm}^{-1}$ ,  $1327\text{ cm}^{-1}$  and  $1240\text{ cm}^{-1}$  confirm the presence of  $\text{CH}_2$  bending, stretching and C–H wagging vibrations, respectively. The characteristic peak observed at  $1085\text{ cm}^{-1}$  can be ascribed to the O–H bending and C–O stretching of an acetyl group [15]. The bands appeared at  $918\text{ cm}^{-1}$  and  $831\text{ cm}^{-1}$  can be ascribed to the skeletal vibration of PVA [22]. The FTIR spectrum of PVA/PEG blend film illustrated in figure 2(b), displays all characteristic peaks of neat polymers. The FTIR bands observed at  $1081\text{ cm}^{-1}$  and  $838\text{ cm}^{-1}$  were ascribed to stretching vibrations of the C–O–C ether linkage and C–C group [23]. The peak at  $3265\text{ cm}^{-1}$  attributing to O–H symmetrical stretching vibration was shifted to  $3269\text{ cm}^{-1}$  in PVA/PEG blend. The peak at  $2939\text{ cm}^{-1}$  ascribing to C–H asymmetric stretching vibration was shifted to  $2916\text{ cm}^{-1}$ . Similarly, the peak at  $1327\text{ cm}^{-1}$  corresponding to  $\text{CH}_2$  stretching vibration was shifted to  $1326\text{ cm}^{-1}$  and another peak at  $1711\text{ cm}^{-1}$  corresponding to the C=O stretching vibration was also shifted to  $1710\text{ cm}^{-1}$ . These shifts in the characteristic peaks towards lower wavelength in FTIR spectra indicate the formation of hydrogen bonding interaction between the O–H groups of polymeric chains [15, 24]. The FTIR spectra of PVA/PEG/CBNPs nanocomposites with various loadings of CBNPs are depicted in figures 2(c)–(e), from which the presence of all the characteristic peaks of PVA and PVA/PEG blend can be identified. The similar characteristics peaks were observed at  $3262\text{ cm}^{-1}$ ,  $1320\text{ cm}^{-1}$ ,  $1081\text{ cm}^{-1}$  and  $830\text{ cm}^{-1}$  with a slight shift towards the lower wavelength indicating the hydrogen bonding formation and the substantial interaction of CBNPs with the polymer blend [4]. Thus, the FTIR results indicate the successful preparation of PVA/PEG/CBNPs nanocomposites.

### Thermogravimetric analysis

The TGA thermographs measuring the weight loss as a function of temperature for PVA/PEG/CBNPs nanocomposites with various loadings of CBNPs are presented in figures 3(a)–(f). As with the increase in temperature, there was a decrease in weight of the sample which indicates the continuous decomposition of the material. In figure 3(a), the TGA thermograph of PVA/PEG blend below  $250\text{ }^\circ\text{C}$  shows nearly 10% weight loss resulting from the evaporation of absorbed water [25, 26]. The decomposition of PVA/PEG blend film held between  $250\text{ }^\circ\text{C}$  to  $450\text{ }^\circ\text{C}$  temperature range with almost 89% weight loss attributing to the abolition of functional groups such as hydroxyl and free amine groups [27]. Further increase in temperature up to  $800\text{ }^\circ\text{C}$ , the 3% weight loss was observed indicating the breaking of carbon chain backbone in the PVA/PEG blend. On adding, CBNPs in the polymer blend, there was a slight decrease in weight loss. The TGA thermographs for CBNPs with 5 wt% loading given by figure 3(b), shows almost 84% weight loss at the temperature ranging from  $250\text{ }^\circ\text{C}$  to  $600\text{ }^\circ\text{C}$  indicating the less weight loss as that of the PVA/PEG blend. Similarly, the weight loss trend was observed for 10 wt% and 15 wt% loadings of CBNPs (figures 3(c), (d)). With further increase in CBNPs loadings, TGA thermographs show two-step decomposition having a significant drop in the weight loss as compared to PVA/PEG blend. The CBNPs loadings with 20 wt% and 25 wt% show a weight loss of almost 52% and 54% respectively, at  $250\text{ }^\circ\text{C}$  to  $450\text{ }^\circ\text{C}$  temperature range attributed to the elimination of functional groups present in the polymer chains [28]. On a further rise in temperature from  $550\text{ }^\circ\text{C}$  to  $800\text{ }^\circ\text{C}$  the weight loss corresponding to 20 wt% and 25 wt% CBNPs loadings were 32% and 27% respectively which could be ascribed to the strong interaction between polymer matrices and the CBNPs [24, 28]. Therefore, the TGA results indicate



a significant decrease in the weight loss by the addition of CBNPs, as compared to the PVA/PEG blend thereby improving the thermal stability of PVA/PEG/CBNPs nanocomposites.

#### DSC measurements

The DSC curves for the PVA/PEG blend and the PVA/PEG/CBNPs nanocomposites with various CBNPs loadings are presented in figure 4. For PVA/PEG blend (figure 4(a)), there are two endothermic peaks detected among which one strong peak is present at 58 °C, whereas the second short but broad peak is present at 220 °C. The endothermic peaks observed for PVA/PEG blend are possibly associated with the melting temperature ( $T_m$ ) of PEG and PVA [29, 30]. Since there is a huge difference between the two temperature values which might be due to the incompatibility of the blend having high PEG (>20 wt%) concentration [31, 32]. The influence of various concentrations of CBNPs on the PVA/PEG blend is represented in figures 4(b)–(e). It was found that with the addition of CBNPs, the single endothermic peak is detected with a significant shift in the  $T_m$ , whereas the width of the peak is almost similar to that of the PVA/PEG blend supporting the single-phase behaviour of polymer blend [33]. Another reason for the shift in the  $T_m$  of PVA/PEG/CBNPs nanocomposites might be the intermolecular interaction between the incorporated CBNPs and the polymer blend indicating the changes



occurring between semi-crystalline and an amorphous phase of the polymers [30, 34, 35]. The  $T_m$  is slightly shifting towards the lower values with the increase in CBNPs content (5 wt%–20 wt%). However, the depth of peak is decreasing with an increase in CBNPs loading and almost vanished for the 25 wt% loading of CBNPs. Also, it can be seen that, as the PEG content decreases the depth of peak also gets lower while no endothermic peak was observed for the nanocomposite containing higher CBNPs loading and in the absence of PEG. The reason for the disappearance of the endothermic peak for 25 wt% CBNPs loading added in the PVA matrix is might be due to the amorphous nature of PVA and there is no significant formation of crystallization in the polymer matrix on adding nanofiller [36, 37]. The endothermic peaks are assumed to be due to the melting of PEG [32]. In addition, the interaction of CBNPs and PEG is strongly attractive as the  $T_m$  is higher than that of 58 °C in nanocomposites [38, 39]. The DSC studies indicate that the PEG and CBNPs have influenced the thermal properties of PVA/PEG/CBNPs nanocomposites.

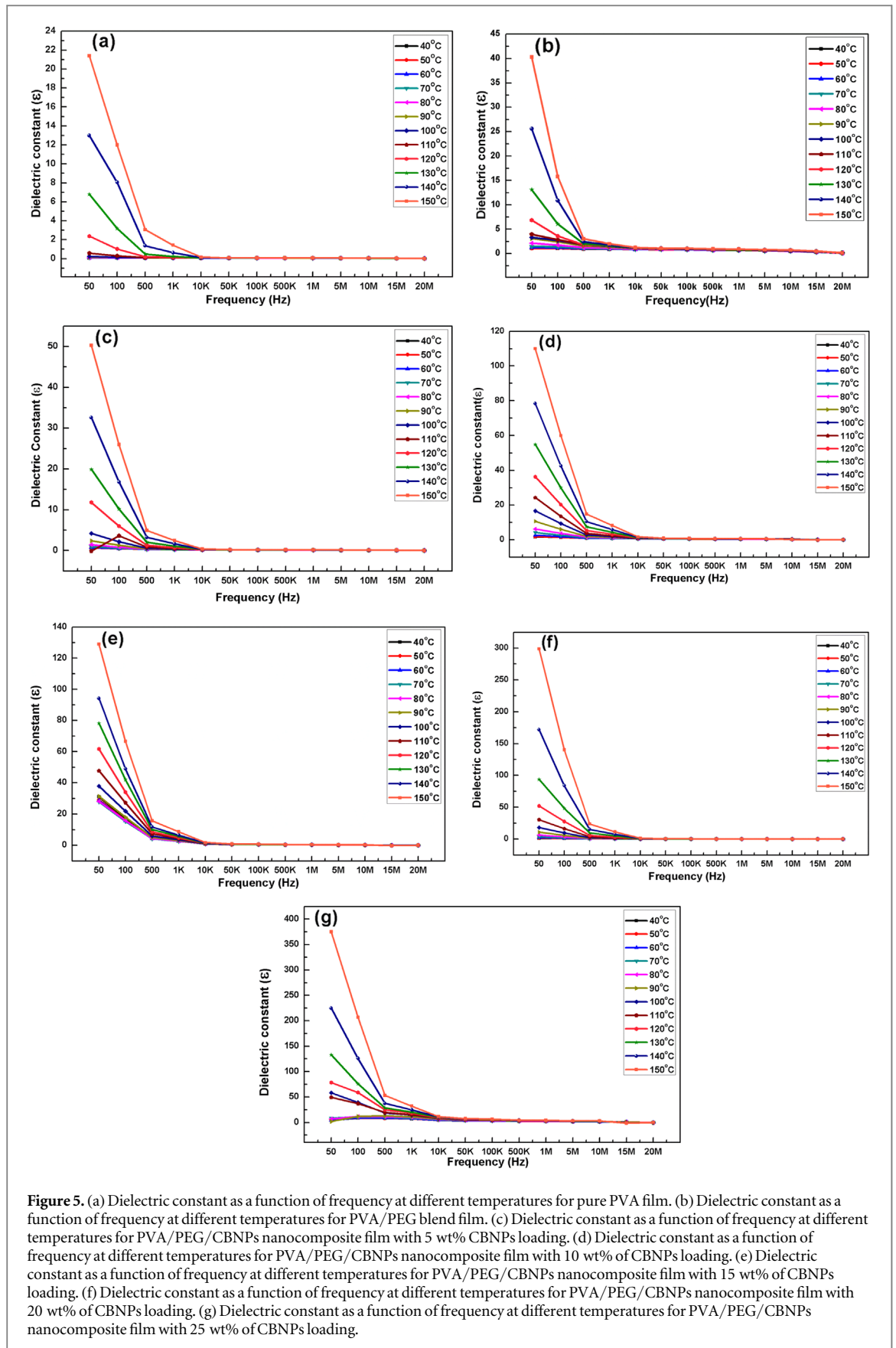
### Dielectric properties

The variation of dielectric properties of CBNPs reinforced PVA/PEG blend nanocomposites in the frequency range 50 Hz to 20 MHz and at temperature range 40 °C to 150 °C were presented in figures 5 and 6. These properties of nanocomposites with various loadings of CBNPs were examined to estimate their feasibility for EMI shielding applications. The maximum values of dielectric constant ( $\epsilon$ ) and dielectric loss ( $\tan \delta$ ) are summarized in table 2. For neat PVA, the maximum  $\epsilon$  shown in figure 5(a) was observed to be 21.4, at 50 Hz and 150 °C. Similarly, for PVA/PEG blend in figure 5(b), the  $\epsilon$  obtained was 40.3 at the same frequency and temperature as that of PVA. In both cases, the maximum  $\epsilon$  was observed at low frequency (50 Hz) and it was decreased swiftly with further increase in the frequency. According to the Maxwell-Wagner-Sillar effect, at low frequency, the maximum  $\epsilon$  values can be attributed to the presence of interfacial polarization [20, 40]. The  $\epsilon$  plots for PVA/PEG/CBNPs nanocomposites with various loadings of CBNPs are depicted in figures 5(c)–(g). On adding nanofiller in the polymer blend, the increment in  $\epsilon$  values was noticed. Generally, the reinforcement of CBNPs as filler in the polymer matrix can reduce the interfacial polarization because of the fillers conformation in the chain length of the polymer matrix [41]. It can be seen in figures 5(c)–(g) that when the filler concentration increases the  $\epsilon$  was increased. For lower concentration (5 wt%) of CBNPs the  $\epsilon$  value was 50.3 and it increases up to 375.1 for higher concentration (25 wt%) of CBNPs. The  $\epsilon$  values are especially higher for filler loadings near to percolation threshold which can be due to the introduction of interlayers within the conductive nanofillers to avoid the current leakage [42]. Furthermore, the  $\epsilon$  values were maximum at low frequency for all the nanocomposites which later decreases sharply with further increase in frequency. This rapid reduction of  $\epsilon$  value in the 50 Hz to 20 MHz frequency range was due to the tendency of dipoles orientation towards the direction of the applied field [43]. Although at high frequency range the dipoles barely orient themselves towards the applied field direction and hence in consequence the  $\epsilon$  values become nearly constant [44].

The  $\tan \delta$  plots of pure PVA, PVA/PEG blend and PVA/PEG/CBNPs nanocomposites are presented in figures 6(a)–(g). The  $\tan \delta$  of pure PVA and PVA/PEG blend was 8.75 (100 Hz) and 9.14 (50 Hz) respectively obtained at 150 °C. Further, on adding CBNPs in the polymer blend, the  $\tan \delta$  increased and the maximum value observed was 20.9 (100 Hz, 140 °C) for the 25 wt% loading of CBNPs. For the CBNPs reinforced PVA/PEG/CBNPs nanocomposites, the  $\tan \delta$  values were observed to be higher as compared to pure PVA. This enhancement was ascribed to the dipole, interfacial charge polarization and the conductivity of the nanocomposites [45]. The higher  $\tan \delta$  values obtained for different CBNPs loadings are mainly ascribed to the continuous network formation in the polymer matrix with the addition of conductive nanofiller [46]. Moreover, the  $\tan \delta$  decreases gradually and becomes nearly constant as the frequency reaches its maximum value (20 Hz). Here, with the introduction of CBNPs the reduction in  $\tan \delta$  with an increase in frequency, was attributed to the restriction imposed on the dipole orientation in the polymer matrix [47]. Therefore, the obtained dielectric results validate the significant control on the percolation threshold attributed to the well-dispersed CBNPs in the polymer blend. The improved dielectric performance of these nanocomposites concludes CBNPs as an ideal nanofillers for the development of high-k materials that can lead to its suitability for flexible, lightweight and low-cost material for EMI shielding applications.

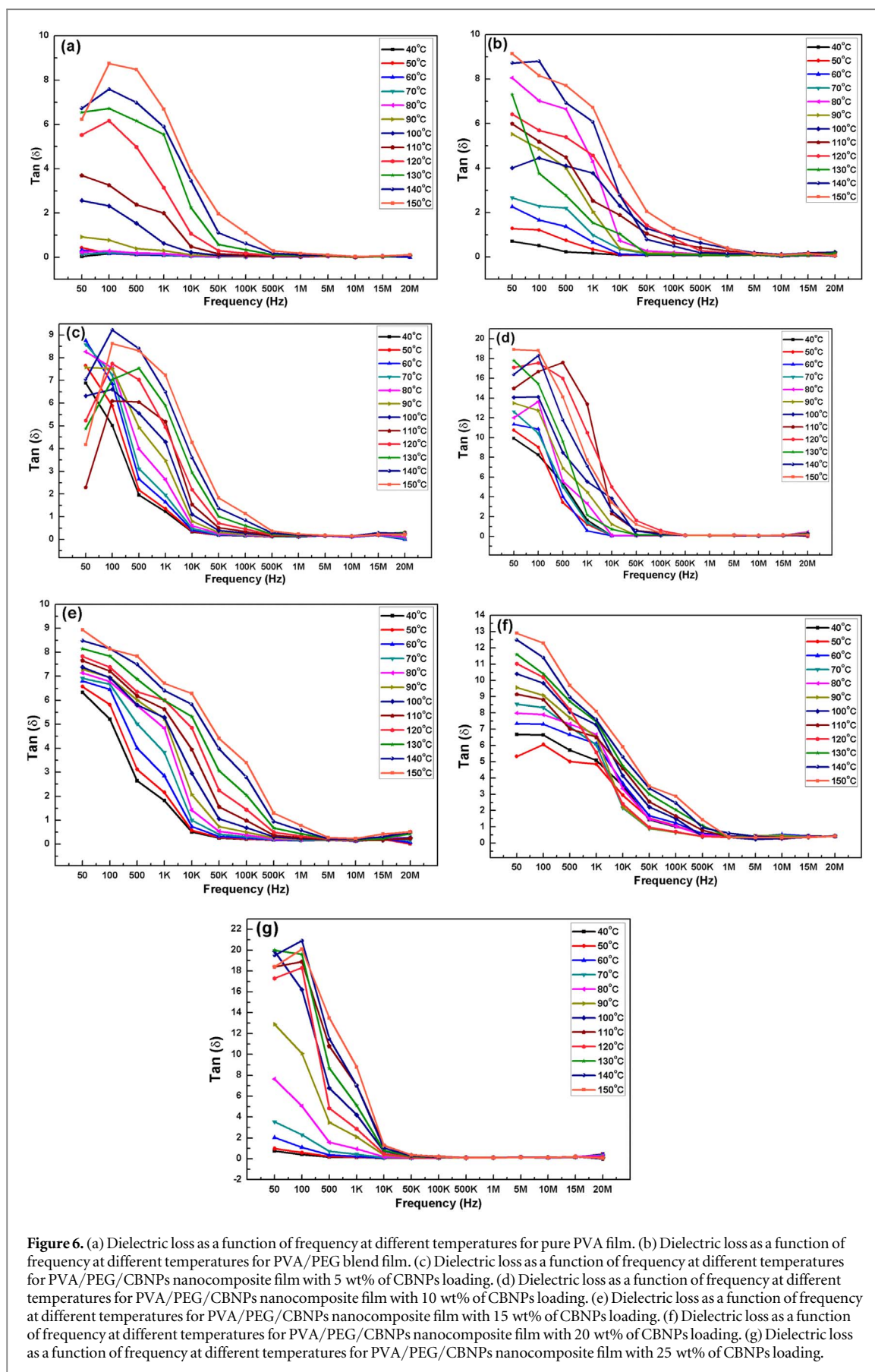
### EMI SE measurements

The EMI SE plots in the Ku-band region (12–18 GHz) for the PVA/PEG blend and the PVA/PEG/CBNPs nanocomposites with various CBNPs loadings are given in figure 7. As depicted in figure 7(a), the PVA/PEG blend shows an EMI SE of 0.1 dB, being entirely transparent to incident electromagnetic radiations exhibiting poor EMI shielding. The poor EMI shielding efficiency refers to the incapability of the polymer blend to form conductive networks [48]. After adding CBNPs in the polymer blend, a significant increase in the EMI SE was observed. Figures 7(b)–(f) presents the EMI SE plots of PVA/PEG/CBNPs nanocomposites with various CBNPs loadings. It was observed that, with the addition of 5 wt% CBNPs loading in the PVA/PEG blend, the EMI SE is



increased up to 1.5 dB. As the CBNPs content was further increased, the EMI SE was significantly increased from 3.6 dB (10 wt% CBNPs) to 8.7 dB (15 wt% CBNPs). This sudden rise in the EMI SE is attributed to the conducting network formation between the CBNPs and PVA/PEG blend. However, the maximum EMI SE attained was about 10.5 dB and 10.6 dB for 20 wt% and 25 wt% loadings of CBNPs respectively. This improved

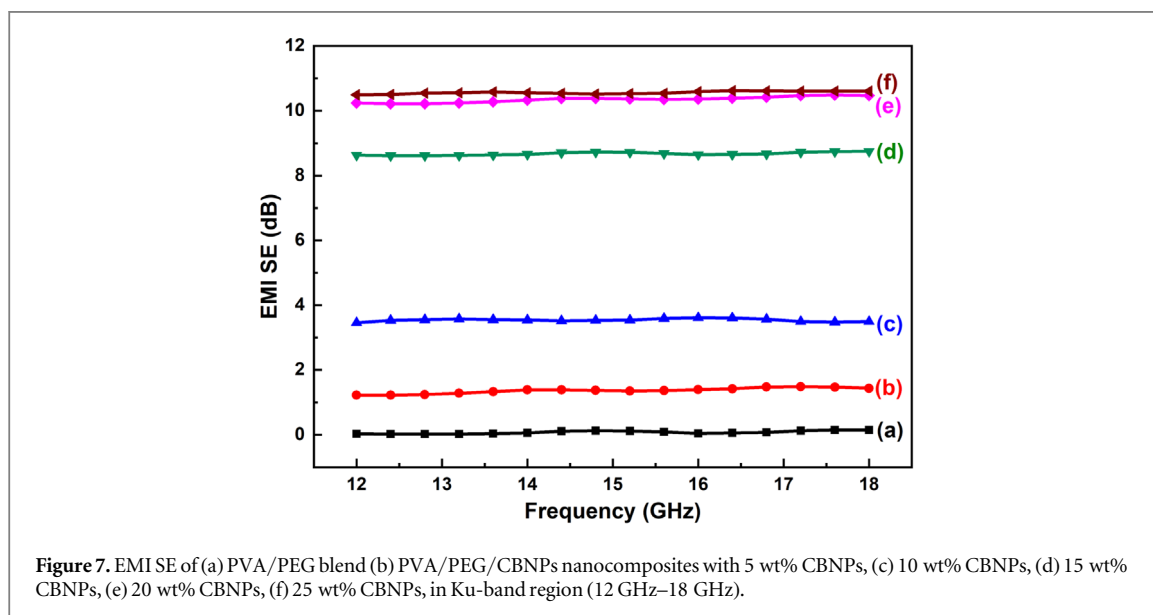




EMI SE emphasized that with an increase in the loadings of CBNPs in the PVA/PEG blend, conductive interconnected networks arise in the nanocomposite, which further signifies the formation of superior interactions between the interfering EM radiations and the nanofiller [49, 50]. According to earlier reports,

**Table 2.**  $\epsilon$  and  $\tan \delta$  values of neat PVA, PVA/PEG blend and the PVA/PEG/CBNPs nanocomposites.

Samples	$\epsilon$	$\tan \delta$
PVA	21.4, 50 Hz, 150 °C	8.75, 100 Hz, 150 °C
PVA/PEG blend	40.3, 50 Hz, 150 °C	9.14, 50 Hz, 150 °C
5 wt% CBNPs	50.3, 50 Hz, 150 °C	9.22, 100 Hz, 140 °C
10 wt% CBNPs	110, 50 Hz, 150 °C	18.92, 50 Hz, 150 °C
15 wt% CBNPs	129, 50 Hz, 150 °C	8.93, 50 Hz, 150 °C
20 wt% CBNPs	299, 50 Hz, 150 °C	12.9, 50 Hz, 150 °C
25 wt% CBNPs	375.1, 50 Hz, 150 °C	20.9, 100 Hz, 140 °C



adding two or more nanofiller in the polymer matrix can significantly enhance their EMI SE [51–53] whereas in this case, CBNPs is the only nanofiller incorporated in the PVA/PEG blend. Furthermore, many studies suggested that by increasing the thickness of the shielding material, a higher value of EMI SE can be achieved [54–57]. However, higher thickness requires a higher concentration of fillers which consequently affects the mechanical strength of the nanocomposite. Therefore, to achieve higher EMI SE at such a lower concentration of nanofiller is still a challenging task.

## Conclusion

In the present work, CBNPs reinforced PVA/PEG blend nanocomposites were synthesized successfully by employing a solution casting method. The FTIR results confirm the occurrence of strong hydrogen bonding interaction between the incorporated nanofiller and the polymer blend. The TGA results indicate significant decrement in the weight loss with the incorporation of CBNPs in the polymer matrix. This decrease in weight loss was attributed to the formation of a strong interface between polymer matrix and the CBNPs thereby improving the thermal stability of PVA/PEG/CBNPs nanocomposites as compared to the PVA/PEG blend. The DSC results reveal the change in  $T_m$  values with the addition of CBNPs in the polymer blend. The incorporation of CBNP in the PVA/PEG blend leads to the significant enhancement in the dielectric constant indicating the homogeneous dispersion of nanofiller within the polymer matrix. The maximum  $\epsilon$  value obtained for neat PVA, PVA/PEG blend and PVA/PEG/CBNPs nanocomposites was about 21.4, 40.3 and 375.1 at 50 Hz, 150 °C respectively. Similarly,  $\tan \delta$  increased from 9.22 to 20.9 for 5 wt% to 25 wt% CBNPs loading respectively. The  $\epsilon$  and  $\tan \delta$  were enhanced at low frequencies for all PVA/PEG/CBNP nanocomposites. These results describe the change in interfacial polarization caused by the reinforcement of CBNPs in the PVA/PEG blend matrix. The EMI SE was improved from 0.1 dB for PVA/PEG blend to 11 dB for PVA/PEG/CBNPs nanocomposites with 25 wt% loading. Thus, the PVA/PEG/CBNPs nanocomposites with improved EMI SE, relatively high dielectric constants and low dielectric loss values make them an attractive material for the EMI shielding applications.

## Acknowledgments

The authors Dr M Basheer Ahamed and Ms. Priyanka Rani would like to acknowledge the Department of Science and Technology- Science and Engineering Research Board (DST-SERB), Government of India, for financially supporting this research work under the sanctioned project number EMR/2016/006705.

## ORCID iDs

M Basheer Ahamed  <https://orcid.org/0000-0002-5156-7803>

## References

- [1] Sankaran S, Deshmukh K, Ahamed M B and Pasha S K K 2018 Recent advances in electromagnetic interference shielding properties of metal and carbon filler reinforced flexible polymer composites: a review *Composites Part A: Appl. Sci. Manuf.* **114** 49–71
- [2] Muzaffar A, Ahamed M B, Deshmukh K and Faisal M 2019 Electromagnetic interference shielding properties of polyvinylchloride (PVC), barium titanate (BaTiO<sub>3</sub>) and nickel oxide (NiO) based nanocomposites *Polym. Test.* **77** 105925
- [3] Sankaran S, Deshmukh K, Ahamed M B, Sadasivuni K K, Faisal M and Pasha S K K 2019 Electrical and electromagnetic interference shielding properties of hexagonal boron nitride nanoparticles reinforced polyvinylidene fluoride nanocomposite films *Polym. Plast. Technol. Eng.* **58** 1191–209
- [4] Mohanapriya M K, Deshmukh K, Chidambaram K, Ahamed M B, Sadasivuni K K, Ponnamma D, AlMaadeed M A A, Deshmukh R R and Pasha S K K 2017 Polyvinyl alcohol (PVA)/Polystyrene sulfonic acid (PSSA)/carbon black nanocomposites for flexible energy storage device applications *J. Mater. Sci.: Mater. Electron.* **28** 6099–111
- [5] Bal S and Samal S S 2007 Carbon nanotube reinforced polymer composites—A state of the art *Bull Mater Sci* **30** 379
- [6] Poveda R L and Gupta N 2014 Electrical properties of carbon nanofiber reinforced multiscale polymer composites *Mater Des* **56** 416–422
- [7] Muzaffar A, Ahamed M B, Deshmukh K, Faisal M and Pasha S K K 2018 Enhanced electromagnetic absorption in NiO and BaTiO<sub>3</sub> based polyvinylidene fluoride nanocomposites *Mater. Lett.* **218** 217–20
- [8] Sohi N J S, Rahaman M and Khastgir D 2011 Dielectric property and electromagnetic interference shielding effectiveness of ethylene vinyl acetate-based conductive composites: effect of different type of carbon fillers *Polym. Compos.* **32** 1148–54
- [9] Bhadra S, Chattopadhyay S, Singha N K and Khastgir D 2008 Improvement of conductivity of electrochemically synthesized polyaniline *J. Appl. Polym. Sci.* **108** 57–64
- [10] Mohanapriya M K, Deshmukh K, Sadasivuni K K, Thangamani G, Chidambaram K, Ahamed M B and Pasha S K K 2019 Enhanced quality factor of polyvinylformal (PVF) based nanocomposites filled with zinc oxide and carbon black nanoparticles for wireless sensing applications *Mater. Today: Proceedings* **9** 199–216
- [11] Abdelaziz M 2015 The effects of carbon nanoparticles on thermal and dielectric properties of bisphenol A polycarbonate *J. Thermoplastic Compo. Mater.* **28** 1–21
- [12] Pawde S M and Deshmukh K 2008 Characterization of polyvinyl alcohol/gelatin blend hydrogel films for biomedical applications *J. Appl. Polym. Sci.* **109** 3431–7
- [13] Reddy P L, Deshmukh K, Tomáš K, Nambiraj N A and Pasha S K K 2020 Green chemistry mediated synthesis of cadmium sulphide/polyvinyl alcohol nanocomposites: assessment of microstructural, thermal, and dielectric properties *Polym. Comp.* **41** 2054–67
- [14] Reddy P L, Deshmukh K, Chidambaram K, Nazeer Ali M M, Sadasivuni K K, Kumar Y R, Lakshmi pathy R and Pasha S K K 2019 Dielectric properties of polyvinyl alcohol (PVA) nanocomposites filled with green synthesized zinc sulphide (ZnS) nanoparticles *J. Mater. Sci.: Mater. Electron.* **30** 4676–87
- [15] Thangamani G J, Deshmukh K, Chidambaram K, Ahamed M B, Sadasivuni K K, Ponnamma D, Faisal M, Nambiraj N A and Pasha S K K 2018 Influence of CuO nanoparticles and graphene nanoplatelets on the sensing behavior of poly (vinylalcohol) nanocomposites for the detection of ethanol and propanol vapors *J. Mater. Sci.: Mater. Electron.* **29** 5186–205
- [16] Deshmukh K, Ahamed M B, Deshmukh R R, Pasha S K K, Chidambaram K, Sadasivuni K K, Ponnamma D and AlMaadeed M A A 2016 Eco-friendly synthesis of graphene oxide reinforced hydroxypropyl methyl cellulose/polyvinyl alcohol blend nanocomposites filled with zinc oxide nanoparticles for high-k capacitor applications *Polym. Plast. Tech. Eng.* **55** 1240–53
- [17] Deshmukh K, Ahamed M B, Sadasivuni K K, Ponnamma D, AlMaadeed M A A, Pasha S K K, Deshmukh R R and Chidambaram K 2017 Graphene oxide reinforced poly (4-styrenesulfonic acid)/polyvinyl alcohol blend composites with enhanced dielectric properties for portable and flexible electronics *Mater. Chem. Phys.* **186** 188–201
- [18] Deshmukh K, Ahamed M B, Deshmukh R R, Sadasivuni K K, Ponnamma D, Pasha S K K, AlMaadeed M A A, Polu A R and Chidambaram K 2017 Eeonomer 200F<sup>®</sup>: a high performance nanofiller for polymer reinforcement- Investigation of the structure, morphology and dielectric properties of polyvinyl alcohol/Eeonomer 200F<sup>®</sup> nanocomposites for embedded capacitor applications *J. Electron. Mater.* **46** 2406–18
- [19] Deshmukh K, Ahamed M B, Sadasivuni K K, Ponnamma D, Deshmukh R R, Pasha S K K, AlMaadeed M A A and Chidambaram K 2016 Graphene oxide reinforced polyvinyl alcohol/polyethylene glycol blend composites as high-performance dielectric materials *J. Polym. Res.* **23** 159
- [20] Deshmukh K, Ahmad J and Hagg M B 2014 Fabrication and characterization of polymer blends consisting of cationic polyallylamine and anionic polyvinyl alcohol *Ionics* **20** 957–67
- [21] Deshmukh K, Ahamed M B, Sankaran S, Pasha S K K, Sadasivuni K K, Ponnamma D and AlMaadeed M A A 2018 Studies on the mechanical, morphological and electrical properties of highly dispersible graphene oxide reinforced polypyrrole and polyvinyl alcohol blend composites *Mater. Today: Proceedings* **5** 8744–52
- [22] Pasha S K K, Deshmukh K, Ahamed M B, Chidambaram K, Mohanapriya M K and Nambiraj N A 2017 Investigation of microstructure, morphology, mechanical and dielectric properties of PVA/PbO nanocomposites *Adv. Polym. Tech.* **36** 352–61
- [23] Deshmukh K, Ahamed M B, Deshmukh R R, Pasha S K K, Sadasivuni K K, Ponnamma D and Chidambaram K 2016 Synergistic effect of vanadium pentoxide and graphene oxide in polyvinyl alcohol for energy storage applications *Euro. Polym. J.* **76** 14–27

- [24] Deshmukh K, Ahamed M B, Deshmukh R R, Bhagat P R, Pasha S K K, Bhagat A, Shirbhate R, Telare F and Lakhani C 2016 Influence of  $K_2CrO_4$  doping on the structural, optical and dielectric properties of polyvinyl alcohol/ $K_2CrO_4$  composite films *Polym. Plast. Tech. Eng.* **55** 231–41
- [25] Deshmukh K, Ahamed M B, Pasha S K K, Deshmukh R R and Bhagat P R 2015 Highly dispersible graphene oxide reinforced polypropylene/polyvinyl alcohol blend nanocomposites with high dielectric constant and low dielectric loss *RSC Adv.* **5** 61933–45
- [26] El-Aassar M R, Elnouby M, Kamal F H, Badawy N A F and Amer S I 2016 Chemical crosslinking of poly (vinyl alcohol)/ poly ethylene glycol with glutaraldehyde nanofibers *Al Azhar Bulletin of Science* **27** 9–17
- [27] Barooah M and Mandal B 2018 Enhanced  $CO_2$  separation performance by PVA/PEG/silica mixed matrix membrane *J. Appl. Polym. Sci.* **46481** 1–12
- [28] Xie Y, Zhang S H, Jiang H Y, Zeng H, Wu R M, Chen H, Gao Y F, Huang Y Y and Bai H L 2019 Properties of carbon black-PEDOT composite prepared via *in situ* chemical oxidative polymerization *Polymers* **19** 61–9
- [29] Mohapatra A K, Mohanty S and Nayak S K 2014 Effect of PEG on PLA/PEG blend and its nanocomposites: a study of thermo-mechanical and morphological characterization *Poly. Comp.* **35** 283–93
- [30] Yang C and Lee Y 2009 Preparation of the acidic PVA/MMT nanocomposite polymer membrane for the direct methanol fuel cell (DMFC) *Thin Solid Films* **517** 4735–40
- [31] Aisida S O, Ahmad I and Ezema F I 2020 Effect of calcination on the microstructural and magnetic properties of PVA, PVP and PEG assisted zinc ferrite nanoparticles *Physica B* **579** 411907
- [32] Falqi F H, Bin-dahman O A, Hussain M and Al-harhi M A 2018 Preparation of miscible PVA/PEG blends and effect of graphene concentration on thermal, crystallization, morphological, and mechanical properties of PVA/PEG (10 wt%) blend *Intern. J. Poly. Sci.* **2018**, 1–10 Article ID 8527693
- [33] Salem K S, Lubna M M, Rahman A F M M and Islam R 2014 The effect of multiwall carbon nanotube additions on the thermo-mechanical, electrical, and morphological properties of gelatin—polyvinyl alcohol blend nanocomposite *J. Compos. Mater.* **49** 1–13
- [34] Jin J, Song M and Pan F 2007 A DSC study of effect of carbon nanotubes on crystallisation behaviour of poly (ethylene oxide) *Thermochim. Acta* **456** 25–31
- [35] Xiang A, Wang H, Liu D, Zhang X and Tian H 2018 Melt processing of high alcoholysis poly (vinyl alcohol) with different polyol plasticizers *J. Polym. Eng.* **38** 659–665
- [36] Lee S, Hong J Y and Jang J 2013 The effect of graphene nanofiller on the crystallization behavior and mechanical properties of poly (vinyl alcohol) *Polym. Intern.* **62** 901–8
- [37] Naebe M, Lin T, Tian W, Dai L and Wang X 2007 Effects of MWNT nanofillers on structures and properties of PVA electrospun nanofibres *Nanotechn.* **18** 225605
- [38] Wang C, Feng L, Yang H, Xin G, Wei L, Zheng J, Tian W and Li X 2012 Graphene oxide stabilized polyethylene glycol for heat storage *Phys. Chem. Chem. Phys.* **14** 13233–8
- [39] Radhakrishnan R, Gubbins K E, Watanabe A, Kaneko K, Radhakrishnan R and Gubbins K E 1999 Freezing of simple fluids in microporous activated carbon fibers Comparison of simulation and experiment Freezing of simple fluids in microporous activated carbon fibers: comparison of simulation and experiment *J. Chem. Phys.* **111** 9058–67
- [40] Joshi G M and Deshmukh K 2016 Study of conjugated polymer/graphene oxide nanocomposites as flexible dielectric medium *J. Mater. Sci.: Mater. Electron.* **27** 3397–409
- [41] Sheheri S Z A, Amshany Z M A, Sulami Q A A, Tashkandi N Y, Mahmoud A H and El-Shishtawy R M 2019 The preparation of carbon nanofillers and their role on the performance of variable polymer nanocomposites *Des Monom Polym* **22** 8–53
- [42] Xu J, Wong M and Wong C P 2004 Super high dielectric constant carbon black-filled polymer composites as integral capacitor dielectrics *Proceedings—Electr. Compo. Techno. Confer.* **1** 536–41
- [43] Pandey M, Joshi G M, Deshmukh K, Khutia M and Ghosh N N 2014 Optimized AC conductivity correlated to structure, morphology and thermal properties of PVDF/PVA/Nafion composites *Ionics* **20** 1427–33
- [44] Krishnakumar V and Shanmugam G 2012 Structural, optical and dielectric properties of Pbs-PVA-PEG nanocomposite film *Sci Adv Mater* **4** 1–7
- [45] Deshmukh K, Ahamed M B, Deshmukh R R, Pasha S K K, Sadasivuni K K, Polu A R, Ponnamma D, AlMaadeed M A A and Chidambaram K 2017 Newly developed biodegradable polymer nanocomposites of cellulose acetate and  $Al_2O_3$  nanoparticles with enhanced dielectric performance for embedded passive applications *J. Mater. Sci.: Mater. Electron.* **28** 973–86
- [46] Joshi G M, Sharma A, Tibrawala R, Arora S, Deshmukh K, Kalainthan S and Deshmukh R R 2014 Preparation and Performance Characterization of Soft Polymer Composites as a Function of Single and Mixed Nano Entities *Polym Plast Technol Eng* **53** 588–595
- [47] Joseph J, Deshmukh K, Chidambaram K, Faisal M, Selvarajan E, Sadasivuni K K, Ahamed M B and Pasha S K K 2018 Dielectric and electromagnetic interference shielding properties of germanium dioxide nanoparticle reinforced poly (vinylchloride) and poly (methylmethacrylate) blend nanocomposites *J. Mater. Sci.: Mater. Electron.* **29** 20172–88
- [48] Mohanapriya M K, Deshmukh K, Kadlec J, Sadasivuni K K, Faisal M, Nambiraj N A and Pasha S K K 2020 Dynamic mechanical analysis and broadband electromagnetic interference shielding characteristics of poly (vinyl alcohol)-poly (4-styrenesulfonic acid)-titanium dioxide nanoparticles based tertiary nanocomposites *Polym-Plast Tech Eng.* **59** 847–63
- [49] Rahaman M, Chaki T K and Khastgir D 2011 Development of high-performance EMI shielding material from EVA, NBR, and their blends: effect of carbon black structure *J. Mater. Sci.* **46** 3989–99
- [50] Taylor P, Vovchenko L L, Matzui L Y, Oliynyk V V and Launetz V L 2011 The effect of filler morphology and distribution on electrical and shielding properties of graphite-epoxy composites *Molec. Cryst. Liq. Cryst.* **535** 179–88
- [51] Al-Saleh M H and Sundararaj U 2008 Electromagnetic interference (EMI) shielding effectiveness of PP/PS polymer blends containing high structure carbon black *Macromol. Mater. Eng.* **298** 621–30
- [52] Bigg D M, Laboratories C and Avenue K 2013 An investigation of the effect of carbon black structure, polymer morphology, and processing history on the electrical conductivity of carbon black filled thermoplastics *J. Rheol.* **28** 501–16
- [53] Li Y, Zhang A, Lu H, Zhang X, Zheng W and Li M 2018 Effect of polar polymers of PEG and PVA on the enhanced microwave-absorbing properties of MWNTs *J. Phys. Chem. C* **122** 16956–63
- [54] Dhakate S R, Subhedar K M and Singh B P 2015 Polymer nanocomposite foam filled with carbon nanomaterials as an efficient electromagnetic interference shielding material *RSC Adv.* **5** 43036–57
- [55] Zhang C, Ni Q, Fu S and Kurashiki K 2007 Electromagnetic interference shielding effect of nanocomposites with carbon nanotube and shape memory polymer *Compo. Sci. Tech.* **67** 2973–80
- [56] Zeng Z, Chen M, Jin H, Li W, Xue X, Zhou L, Pei Y, Zhang H and Zhang Z 2016 Thin and flexible multi-walled carbon nanotube/waterborne polyurethane composites with high-performance electromagnetic interference shielding *Carbon* **96** 768–77

- [57] Zhang X, Zhang X, Yang M, Yang S and Wu H 2016 Ordered multilayer film of (graphene oxide/polymer and boron nitride/polymer) nanocomposites: an ideal EMI shielding material with excellent electrical insulation and high thermal conductivity *Compos. Sci. Technol.* **136** 104–10